HHS Public Access

Author manuscript

*Nat Chem Biol*. Author manuscript; available in PMC 2011 September 01.

Published in final edited form as:

*Nat Chem Biol*. 2011 March ; 7(3): 147–153. doi:10.1038/nchembio.511.

# NMR Analysis Demonstrates Immunoglobulin G *N*-glycans are Accessible and Dynamic

**Adam W. Barb** and **James H. Prestegard***

Complex Carbohydrate Research Center, 315 Riverbend Road, University of Georgia, Athens, Georgia 30602

## Abstract

The *N*-glycan at Asn297 of the Immunoglobulin G Fc fragment modulates cellular responses of the adaptive immune system. However, the underlying mechanism remains undefined as existing structural data suggest the glycan does not directly engage cell surface receptors. Here we characterize the dynamics of the glycan termini using solution nuclear magnetic resonance (NMR) spectroscopy. Contrary to previous conclusions based on x-ray crystallography and limited NMR data, the spin relaxation studies presented indicated the termini of both glycan branches to be highly dynamic and experiencing considerable motion in addition to tumbling of the Fc molecule. Relaxation dispersion and temperature-dependent chemical shift perturbations demonstrated exchange of the α1–6Man-linked branch between a protein-bound and a previously unobserved unbound state, suggesting the glycan samples conformational states that can be accessed by glycan modifying enzymes and possibly glycan recognition domains. These findings suggest a role for Fc-glycan dynamics in Fc:receptor interactions and enzymatic glycan remodeling.

As a primary component in the second phase of the adaptive immune system, Immunoglobulin G (IgG) binds to foreign particles in the blood and targets these invaders for destruction. IgG engaged with an antigen triggers this process by interacting with cell surface receptors and the C1q component of complement through its Fc domain1. Specific recognition of IgG then leads to localized inflammation by activating the immune system; this activation threshold must be balanced to avoid hyposensitivity to foreign particles and hypersensitivity to autoantigens. Either extreme results in serious disease, enhanced sensitivity to infection on one hand and debilitating autoimmune disease on the other hand2. There is good reason to believe that the carbohydrates attached to the Fc fragment play a role in maintaining this balance in sensitivity3 and that understanding the conformation and conformational excursions of the glycans could help in the design in appropriate modulators of immune sensitivity. NMR studies presented here take a step toward that understanding.



*Corresponding Author: jpresteg@ccrc.uga.edu, Phone 706-542-6281, Fax 706-542-4412.

Author Contributions

A.W.B. and J.H.P. designed experiments, analyzed data and wrote the manuscript.

A.W.B. performed experiments.

Competing Financial Interests

A.W.B. and J.H.P declare no competing financial interests.

IgG Fc from healthy humans has a complex-type biantennary *N*-glycan attached to Asn297 of the Cγ2 domains of the dimeric Fc fragment (see Figure 1)3. While the Fc glycans are quite heterogeneous, a high percentage is normally terminated with galactose. Deviations from this pattern correlate well with certain diseases as well as differential effects on inflammatory response4. For example, in those suffering from rheumatoid arthritis (RA), a crippling autoimmune disorder, these glycans are mostly ungalactosylated leaving *N*-acetylglucosamine residues at the termini of one or both branches of the glycans5. Recent studies also show that the Fc fragment, once enzymatically sialylated in vitro, is potently anti-inflammatory and reduces RA disease severity in a mouse model6,7. This observation has significant implications for possible improvements in intravenous IgG therapy for patients suffering from severe cases of RA by enzymatically adding sialic acids to the normal glycan termini of pooled IgG7. Other correlations between glycan compositions and Fc interactions with its receptors have also been noted6,8–11. In the case of the anti-inflammatory activity of Fc with sialylated glycans, a specific receptor has been postulated12, but, it is not clear how changes in glycan composition modulate interactions with receptors.

Our current structural knowledge of Fc and its glycans is actually quite substantial, but this has done surprisingly little to resolve question regarding glycan modulation of receptor interactions. For example, in x-ray diffraction derived models of Fc – receptor complexes13–15 the glycans do not directly interact with the surface of the receptors and glycan modifications seem to induce little change in Fc geometry near the interaction site9. The ends of IgG Fc glycans in galactose terminated cases are well resolved in several x-ray diffraction-derived models and appear to be buried between two Cγ2 domains16,17, leaving their accessibility for any sort of interaction in question. Solution NMR measurements of the same Fc glycoform indicated that the α1–6Mannose (Man) branch was completely immobilized through interactions with the protein surface while the α1–3Man terminus was more dynamic18,19. Immobilization presumably would strongly restrict the α1–6Man branch terminus in interactions with receptors and glycan modifying enzymes such as the sialyltransferases and glycosidases (neuraminidase, β-galactosidase, *N*-acetylglucosaminidase). It would also indirectly restrict the α1–3Man branch in these same interactions.

Despite these inferences from structural data, glycan termini have been remodeled in vitro using various enzymes6,18,20,21. Attempts to add sialic acids to branch termini of Fc domains using human sialyltransferase St6GalI21 suggest a strong preference for addition to the more dynamic α1–3Man branch. However, the sialyltransferase prefers the α1–3Man galactose over the α1–6Man galactose even using isolated glycans, with this preference only moderately enhanced using Fc-conjugated glycans. Thus, there is an apparent contradiction between the current structural picture of tight coordination of galactose-terminated glycans and the availability of the glycan termini to various glycan modifying enzymes. This provides motivation for the study presented here using solution nuclear magnetic resonance (NMR) spectroscopy to study dynamic sampling of other glycan conformations.

Solution NMR spectroscopy is an ideal technique for the characterization of the structure and dynamics of conformationally labile systems22. Polysaccharides themselves are

conformationally labile due a lack of short or long range stabilizing interactions. This has often made their study by purely structural methods difficult. Terminal residues of glycans are often unresolved in x-ray crystal structures of glycoproteins either because of conformational heterogeneity or because of enzymatic truncation to improve crystallizability23,24. Even when observed, one must remember that the conformations seen may represent only one low energy conformer of an ensemble of structures accessible in solution. In contrast to x-ray diffraction, all members of a conformationally labile moiety often contribute to observable NMR parameters.

Using NMR, the timescales, and sometimes amplitudes of motion in carbohydrates, can be characterized based on well-defined spin relaxation techniques and theory25,26. Current applications of NMR spin relaxation techniques have been developed primarily for observation of backbone amide or sidechain methyl groups in studies of dynamics in isotopically labeled proteins25–27. Techniques to label, assign, and characterize the dynamics of glycoprotein glycans are less well developed (reviewed in ref24). Here we present methods to incorporate $^{13}C$ labels into glycoproteins and assign the resonances using a combination of enzymology, mass spectrometry and solution NMR spectroscopy. NMR pulse sequences specific for the resulting labeling schemes are also reported that can be used to address a number of challenges in glycoprotein structural biology. Using these methods, we here report on the dynamics and probable structure of the residues at the termini of Fc glycans.

## Results

### Isotope labeling of IgG glycans

To selectively enhance the signals from the IgG N-glycans, we added $^{13}C$-enriched galactose residues to the glycan termini of intact IgG1 from myeloma cells. A two dimensional $^{1}H$-$^{13}C$ correlation experiment (a heteronuclear multiple quantum coherence (HMQC) spectrum) showed two sets of resonances, a stronger set and a weaker set (Figure 2**a**). The origin of the two sets was further investigated by separating the Fc and Fab fragments using proteolysis of the IgG1 molecule followed by preferential retention of the Fc fragment on an affinity column. A similar two-dimensional spectrum of the non-retained fraction (Figure 2**b**) showed the more intense set of resonances to belong to the Fab fragment. Despite the lack of a consensus N-glycosylation site on the constant regions of IgG Fab fragments, ~30% of circulating IgGs contain an N-glycan attached to the variable region of the molecule28, and higher glycan mobility at these glycosylated sites likely allows these to be detected with more intensity. An experiment using purified Fc fragment (Figure 3**a**) also showed the less intense signals observed in the IgG1 spectrum. It is interesting to note that the resonances appeared in the same position when using the intact IgG1 molecule and the isolated fragments; however, lineshapes were sharper and signals more intense in spectra of the smaller fragments. These data suggested the presence of the Fab fragment did not affect the chemical environment of the Fc glycan, allowing studies of Fc fragment resonances in the isolated fragment.

We, therefore, investigated the Fc glycan more thoroughly using Fc fragments prepared from pooled human serum. Figure 3**a** shows a $^{13}C$- HMQC spectrum for a sample of IgG-Fc

labeled with uniformly $^{13}$C-enriched galactose at the termini of both branches of its glycans. This spectrum clearly showed two types of resonances, one broad set and one sharp (the broad set was less easily observed in the intact IgG molecule of Figure 2**a** because of the additional line broadening due to its larger size). The difference in the two sets for the Fc sample was more clearly shown in a spectrum of Fc fragments labeled with galactose enriched at just the $C_2$ position (Figure 3**b**). This labeling allowed specific assignments of the $C_2$ carbon resonances and permitted examination of linewidths in cross-sections from rows through the two peaks (see insert in Figure 3**b**).

To obtain branch specific assignments we prepared an Fc fragment enriched primarily on the α1–6Man terminus with $^{13}C_U$-galactose. We first introduced unlabeled galactose residues at the termini of the Fc glycan, which natively are not fully galactosylated on either the α1–6 or α1–3Man branch and are seldom sialylated, then sialylated the glycans using St6Gal1 which placed a sialic acid residue preferentially on the α1–3Man branch21. Exogalactosidase treatment then removed the α1–6Man branch galactose but failed to remove the largely unlabeled α1–3Man galactose as it was protected by the sialic acid. Finally, we galactosylated the glycans with uniformly $^{13}$C-labeled galactose on the α1–6Man branch terminus (see Methods). The resulting spectrum is shown in Figure 3**c**. The sharper set of peaks was much reduced in intensity in comparison to Figure 3**a**, allowing assignment of these peaks to the α1–3Man branch and the broad peaks to the α1–6Man branch. This assignment is consistent with previous observations which identified a broad galactose anomeric resonance as the α1–6Man galactose of the Fc-conjugated glycan18.

A comparison of our spectra to the chemical shifts of a free glycan and free galactose revealed the atom-specific identities of these peaks (ref 29–31, Biological Magnetic Resonance data Bank: www.bmrb.wisc.edu). The chemical shift pattern of the α1–3Man branch resonances was quite similar to that reported in the literature for isolated glycans of similar structure; however, all resonances were shifted slightly downfield in both $^1$H and $^{13}$C dimensions. In contrast, the α1–6Man branch resonances experienced significant deviations when compared to a free glycan. The anomeric resonances of the α1–3 and α1–6Man branches (not shown in Figures 2 and 3) had the least similar chemical shift values, followed by the 2 position; the remaining positions had more similar shifts (Supplementary Results, Supplementary Figure 1).

## Dynamics of IgG glycans

NMR resonance linewidths, which are directly related to transverse relaxation rates ($R_2$s), provide a very ready measure of dynamic properties with narrower lines indicating decreased relaxation rates and increased rates of rotational motion. Figure 3 shows that the proton linewidth of the $H_2$ resonance of the α1–6Man branch was nearly twice that of the corresponding resonance from the α1–3Man branch. This immediately suggested the α1–6Man branch to be more immobilized. $^{13}$C linewidths can be more quantitatively interpreted because the dominant relaxation mechanisms can often be assumed to originate in the dipole-dipole interaction with directly bonded protons. Previous work on $^{13}$C spin relaxation had in fact interpreted linewidth data of the Gal $C_1$s[18]. This linewidth was very close to that for protein $^{13}$C αs and suggested an interaction between the α1–6Man branch and the

protein strong enough to completely immobilize the branch for periods longer than the protein tumbling time (~20ns). However, at higher fields the $^{13}C$ line widths of the α1–6Man $^{13}C_2$ resonance in our construct were more than 3 times that of the corresponding carbon on the α1–3Man branch (Supplementary Figure 2) and a simple interpretation using an isotropic model gave an effective correlation time of 37ns, a time considerably longer than the hydrodynamic predictions for the Fc fragment.

These anomalies were confirmed in a more complete set of spin relaxation measurements (Figure 4 and Table 1). There was, in fact, field dependence to simple $R_2$ measurements with a smaller relaxation rate observed at 14.0T as opposed to 21.1T. However, $R_1$ measurements, even at this lower field were not consistent with predictions based on an isotropic tumbling model and suggested that if solely dipolar in origin, $R_2$ would be even less at this field strength. Both the field dependence and these inconsistencies suggested contributions to $R_2$ from chemical exchange mechanisms that originate from the α1–6Man branch sampling multiple conformational states on the μs to ms timescale and modulating chemical shift in this process. At least some of the states would have to have substantial internal motion to raise the effective $R_1$ value.

Fortunately, there are good experiments to explicitly probe the existence of chemical exchange contributions. One involves the use of relaxation dispersion experiments in which transverse relaxation rates are measured with Carr-Purcell-Meiboom-Gill pulse sequences having variable delays between 180° pulses (equivalently having variable pulsing rates ($\nu_{CPMG}$))26,27. In these experiments, resonances that experience multiple chemical environments on a timescale near $\nu_{CPMG}$ become less intense at slow pulsing rates and more intense at higher rates. Results from these experiments at 50°C with a field strength of 21.1T or 18.8T are presented in Figure 5**a**. At low pulsing rates the measurements approach predictions from line widths. At higher pulsing rates chemical shifts are rapidly refocused and, in the limit of very rapid pulsing the effects of chemical exchange, are removed. It is significant that the $R_2$ value for the α1–6Man branch fell off with pulsing rate, while the $R_2$ value for the α1–3Man branch did not. The change in $R_2$ in the presence of chemical exchange between two states (state A and state B) was well described by Eq (1) in which the contribution of chemical exchange to the observed $R_2$ is dependent upon the rate of exchange, the time between pulses, and the scaling factor $\phi_{EX}$. Fitting this equation to data for the α1–6Man branch yielded an effective exchange constant of 5300 ± 1700 $s^{-1}$. The scaling factor $\phi_{EX}$ in principle can yield information about the nature of the exchange process by describing populations of states and chemical shift changes on moving between these states. But these factors are not easily separated without additional information.

The effect of chemical exchange rates on $R_2$ can also be investigated with $R_{1\rho}$ measurements. In low and moderate locking fields, $R_{1\rho}$ should approach the non-exchange contribution to $R_2$ ($R_2^o$). $R_{1\rho}$ for both the α1–6Man branch and the α1–3Man branch did in fact approach the rapid pulsing limit of $R_2$ from the CPMG experiments (Figure 5 and Table 1). The large deviations from $R_2$ based on the linewidth for the α1–6Man branch was clearly consistent with large chemical exchange contributions. There was a smaller but significant deviation from $R_2$ based on the linewidth for the α1–3Man branch. This was not seen in the

CPMG experiments suggesting that there may be some small exchange contributions at a faster rate not accessible with CPMG experiments for this branch.

## Bound-state properties of IgG glycans

Ideally one would like to characterize the conformations involved in exchange processes more thoroughly. Traditional NMR techniques involving the measurement of distance-dependent NOEs or scalar couplings were unsuccessful, likely due to the dynamic nature of these glycans (data not shown) and the tendency of glycan interactions to be mediated by hydrogen bonds from exchangeable hydroxyl protons rather than the protons attached to carbons. Dynamic sampling of multiple states reduces NOEs involving carbon-bound protons from any one state, and under solvent conditions used here, un-observable deuterons replaced hydroxyl protons. While in principle, the relaxation dispersion experiments provided some structural information in terms of a product of fractional populations and chemical shift deviations squared, additional information was needed to separate these factors.

One can in fact use the temperature dependence of the α1–6Man galactose chemical shifts, along with some assumptions about the nature of exchange to provide some of this information. The Fc fragment is thermostable and permits measurements across a wide temperature range with the first of three unfolding events occurring with a $T_m$ >70°C32. Our observations indicated the chemical shifts of the Fc α1–6Man galactose residues were quite sensitive to temperature. Among these, the $^{13}C_2$ resonance showed the greatest displacement in the 5–50°C range with a chemical shift value that approached a plateau of 75.3 ± 0.2 ppm at the high temperature limit (Figure 5b). The plateau value, representing state A, was reasonably consistent with chemical shift values for the same site in the free glycan. While this analysis focused on the $C_2$ carbon, it is significant that several other resonances showed similar trends and moved from a perturbed resonance position at lower temperature toward a free glycan position at higher temperatures.

Using the more precisely determined chemical shift of state A (Figure 5**b** and Table 2) in conjunction with the observed chemical shift at 50°C (Figure 3**a,b**) and the CPMG relaxation dispersion data (Figure 5**a**) we extracted a value for the population of state A ($p_A$) of 0.8 using Eq (4). The value of $p_A$ may then be used to deconvolute $\phi_{EX}$ and derive a value for Δω using the relationship in Eq 2. The state B chemical shift of 76.4 ±0.5 ppm was determined using the resultant value for Δω of 1500 ± 300 rad $s^{-1}$ along with the state A chemical shift.

The temperature-dependent chemical shift data alone may be analyzed to provide an independent measure of population changes as well as the state B chemical shift, as long as one can access a reasonable range of fractional population ($0.2> p_A p_B > 0.1$) and the chemical shift difference (Δω) is relatively large. The data in Figure 5**b**,fit with Eq (3), show the chemical shift at the low (state B) temperature limit and gave ΔH and ΔS values (Table 2). Despite the limited fractional population range, these values were in good agreement with those determined using the CPMG data. The data indicated that populations were approximately equal at 15°C and moved to higher populations of state A (the state with shifts similar to a free glycan) at temperatures above 15°C. At 37° state A was

approximately 70% populated. The trend was consistent with a large positive ΔS value and a significant distribution of sampled conformations in state A.

Assuming that we have properly removed effects of chemical exchange, it is of some interest to assess the internal dynamics of the galactose residues at the ends of the two branches. For the α1–6Man branch this can be done by determining the order parameter (*S*) and the internal motion correlation time ($\tau_e$) that characterize the motion of the galactose $^{13}C_2$-H bond vectors relative to the Fc polypeptide in the un-bound state. This can be done using the Lipari-Szabo formalism33,34 and $R_1$ and $R_2^o$ values corrected for contributions of the bound state assuming isotropic tumbling of Fc at its hydrodynamic limit. Order parameters range from 0 to 1, with 0 corresponding to unrestrained excursions and 1 corresponding to a completely immobilized state. The value for *S* of the $^{13}C_2$-H bond vector was 0.3, suggesting this vector is allowed considerable motional excursions relative to the Fc polypeptide. The value of $\tau_e$ was 2 ns. This was considerably shorter than the correlation time characterizing Fc tumbling indicating a high degree of flexibility. Motions of the α1–3Man branch can be analyzed in a similar fashion, but without having to correct $R_1$ and $R_2^o$ values for a bound state. The order parameters and internal correlation time were 0.4 and 2 ns suggesting similar degrees of conformational sampling and levels of flexibility for both branches when in an unbound state.

## Discussion

Prior X-ray structural data and NMR dynamics analysis had clearly led to the impression that glycans attached to the Fc fragment of IgG are both occluded within a cavity between the halves of the dimeric structure and that the α1–6Man branch of the glycan was firmly anchored to the protein surface. IgG structures are in fact one of a small number of glycoprotein structures showing discrete electron density from extended parts of attached glycans. The existence of a protein-bound state of this glycan branch has been accepted beginning with the first high-resolution structure of the Fc fragment17. Prior studies of the Fc glycan using solution NMR concluded that the α1–6Man branch terminus was firmly bound to the protein surface based on one-dimensional $^1$H spectroscopy measurements of relaxation rates, or the use of linewidths from one-dimensional $^{13}$C spectroscopy to estimate these rates18,19. The examination here, based on multiple field studies and an extended set of spin relaxation experiments, leads to a somewhat different picture that may be more consistent with other biochemical data. Our prior work on sialylation of human IgG Fc, as well as other previous work on IgG Fc, shows that at least the galactose terminated α1–3Man branch is readily accessible for enzymatic addition of sialic acid11,21,35. Our work suggests rates of addition are attenuated by approximately a factor of five by attachment of the glycans to the protein21. It was also shown that the preferential addition to the α1–3Man branch is not solely a result of attachment of the glycan to Fc, but is inherent in enzyme specificity observed even when using free glycan as the substrate. There have been some mutational studies supporting specific interactions between residues on the proteins and the glycan. Interestingly, the proposed polypeptide interactions, notably through Phe241 and Phe243, inhibit but do not prevent glycan processing32,36.

Based on data presented here the α1–3Man branch showed substantial levels of internal motion and chemical shift patterns that well approximate those of the free glycan (Supplementary Figure 1**c**), though all resonances were shifted slightly downfield. Both suggested nothing more than minimal interactions of at least the terminal galactose with the protein surface. This could be consistent with multiple conformers that populate the cavity in the Fc crystal structure. Terminal residues on this branch do not usually give sufficient electron density to allow definitive modeling. However, the data presented here, as well as the previous enzymatic data are more consistent with conformational excursions that fully expose the terminus of the α1–3Man branch.

Data for the α1–6Man terminus of the Fc glycan also showed substantial mobility with excursions between at least two distinct states. The time scales of these excursions (~5000 $s^{-1}$) and the populations of the states would be adequate to allow access to enzymatic modification with reductions in efficiency entirely consistent with observation. The chemical shifts estimated for the two states of the α1–6Man branch of the glycan support a transition between something similar to that observed in crystal structures (pdb - 1l6x[16], 1dn2[37]) and one that is more fully exposed. The dominant, high temperature, state again has chemical shifts approaching those of a free glycan. This would be consistent with a more exposed structure.

We can rationalize chemical shift changes based on existing crystal structures. The high resolution Fc structures with low temperature (B) factors for the α1–6Man linked terminus (pdb -1l6x, 1dn2) have glycosidic torsion angles φ and ψ for the α1–6Man linked galactose-*N*-acetylglucosamine unit of ~65° and ~11°, respectively, which are close to the values of 55° and 6°, respectively, for a calculated energy-minimized structure and 45° and 15°, respectively for the crystal structure of methyl-β-D-lactoside38. This observation is consistent with the general conservation of the α1–6Man linked terminus structure between a protein coordinated and an uncoordinated state, suggesting the large chemical shift deviations characterizing the low-temperature state of the glycan are due to interactions with the protein surface rather than changes in internal conformation of the glycan. Resonances at the 1, 2 and 3 positions of the galactose ring experienced the greatest deviation in chemical shifts (Supplementary Figure 1**a**). This is consistent with the proximity of this portion of the carbohydrate to a surface cavity observed in high resolution Fc models (pdb 1l6x, 1dn2). The 4,5 and 6 positions, however, saw less chemical shift deviations and are located away from the cavity. Therefore, we interpret the minor, low temperature state (B) of the α1–6Man galactose residue as one bound to the surface of the Cγ2 domain in a manner quite consistent with crystal structures.

The precise origin of the chemical shift perturbations in state B are difficult to deduce. There are both residues carrying aromatic sidechains and charged side chains in the region of binding. The aromatic residues are known to restrict glycan processing from mutational studies32,36, however, the shifts of the $C_2$ and $H_2$ resonances, which are in opposite directions are not consistent with remote group effects from the phenyl rings; these would be expected to produce shifts in the same direction. Electrostatic effects are more likely; an electric field from a properly positioned positively-charged residue, for example, would be expected to pull electron density onto the $H_2$ proton and away from the $C_2$ carbon producing

shifts in the opposite direction. Lys246 is in a position where it could produce such effects and is part of the galactose binding pocket.

In accordance with the spin relaxation data and chemical shift estimates we propose a much more dynamic model of the glycans on the Fc fragment of IgG as depicted in Figure 6. State B is represented by the X-ray structure of the Fc fragment (pdb-1l6x) with the α1–3Man branch built out in an arbitrary way beyond the branching Man residue. The α1–6Man branch remains fixed in the bound state as seen in the crystal structure. State A (the free state) is represented by structure A. Here only the linkage of the glycan to the N of Asn297 is as in the X-ray structure. The conformation of both branches are extended but in different conformations in the two structures to indicate additional motion of both branches. The location of the dynamic α1–3Man terminus in states B and A, as well as the α1–6Man terminus in A, is purely speculative; however, a location proximal to the face of the Fc fragment as shown in Figure 6 would expose a larger portion of the glycan if the relative location of the two Cγ2 domains as observed from x-ray diffraction data is retained between all states.

These models are consistent with observations in many respects. The glycan is shielded by the Fc polypeptide accounting for some reduction in rates of modification by glycan modifying enzymes, but still accessible, especially in state A. Glycan – polypeptide interactions, notably through Phe241 and Phe243, inhibit but do not prevent glycan processing32,36. In the models the glycan in the B state is shielded by these residues as highlighted in Figure 6 potentially accounting for the observations.

The labeling, assignment and pulse techniques reported here surmount the many challenges facing protein-conjugated glycan studies and are applicable to a wide range of glycoprotein systems, though further methodological improvements will be required for more complex systems. These methods will be central to studying the association of the Fc fragment with cell-surface receptors and characterizing the role the glycans play in these interactions.

## Methods

### Materials

All enzymes and chemicals were purchased from Sigma-Aldrich (St. Louis, MO), unless otherwise noted. $^{13}C_U$-galactose, $^{13}C_2$-galactose and deuterium oxide ($D_2O$) were from Cambridge Isotopes (Cambridge, MA), the Fc fragment of IgG and IgG1 was from Athens Research and Technologies (Athens, GA).

### Remodeling the IgG1 and IgG Fc glycans

The Fc fragment and IgG1 glycans were remodeled with $^{13}$C-galactose and *N*acetylneuraminic acid as previously described21. IgG1 proteolysis was performed using 2 mg / mL papain activated for 10 min at 37°C in a buffer containing 1 mM EDTA, 10 mM cysteine and 50 mM sodium phosphate, pH 7.0. This mixture was washed in a 10kDa-cutoff centrifugal filter (Millipore) to exchange the buffer with 25mM sodium phosphate, 100 mM potassium chloride, pH 7.0. Activated papain (0.1mg) was incubated with 10 mg IgG1 for 4 h at 37°C. Fc and Fab fragments were separated using a Protein A-sepharose column (GE

Healthcare) to retain the Fc fragment. Following a complete digestion as judged by sodium dodecyl sulfate poly acrylamide gel electrophoresis, the Fab fragments were pooled from the column flow through plus wash fractions and the Fc fragment was recovered in fractions eluted with a buffer containing 0.1M glycine, pH 3.0.

Fc fragment (10 mg) with $^{13}C_U$-galactose enrichment on the α1–6Man branch of the glycan was prepared by first removing existing galactose and *N*-acetylneuraminic acid residues with 80 units β-galactosidase and 250 units sialidase (New England Biolabs) in a 3 mL reaction containing 50 mM Tris, 200 mM sodium chloride and 0.05% sodium azide, pH 8.0. The Fc fragment was then purified over a Protein A-sepharose column, dialyzed against a buffer containing 10 mM MOPS, pH 7.2, then lyophilized. Galactosylation and sialylation were completed as described21 using $^{12}C_U$ sugar nucleotides. Following the four day sialylation reaction, the protein was exchanged into a buffer containing 50 mM sodium citrate, 100 mM sodium chloride and 80 units β-galactosidase, pH 6.0. After an overnight incubation at 37°C, Fc was again purified over a Protein A –sepharose column to remove the exoglycosidase. Following dialysis and lyophilization, Fc was incubated with β1–4galactosyl transferase and UDP-$^{13}C_U$-galactose for two days at 37°C. The completion of the reactions was confirmed by MALDI-MS analysis of the released glycans21.

## NMR spectroscopy

NMR spectroscopy was performed on spectrometers operating at 21.1T, 18.8T or 14.0T. The 21.1T instrument was equipped with a Varian VNMRS console and 5 mm cryogenically-cooled probe with a cold carbon preamp suited for direct $^{13}C$ observation. One 14.0T machine had a similar arrangement with a 3 mm cryogenically-cooled probe. The other 14.0T and the 18.8T instruments were equipped with a Varian Inova console and a 5 mm cryogenically-cooled probe. For each experiment, the temperature was calibrated with an ethylene glycol standard under conditions approximating data acquisition. Once the instrument temperature had equilibrated and the shimming had stabilized acquisition was initiated. DSS was included as an internal reference in each sample. Additionally, the DSS methyl linewidth was measured before and at the end of each experiment (< 1 Hz) to establish field heterogeneity contributions to glycan resonance linewidths.

NMR samples consisted of 2–10 mg of protein in 100% $D_2O$ buffer containing 25 mM sodium phosphate, 100 mM potassium chloride and 1 mM DSS, pH 7.0. Samples were degassed using a vacuum pump until no bubbles were formed. CD spectroscopy and $^1H$ NMR confirmed the samples were folded (data not shown).

A standard $^{13}C$ heteronuclear single-quantum coherence (HSQC) experiment (Varian Biopack) was modified to measure the spin relaxation rates of galactose $^{13}C_6$ by specifically transferring magnetization to $C_6$ and decoupling $C_5$ from $C_6$ during $R_2$ measurement (see Supplementary Methods, Supplementary Figure 3). This is possible at high magnetic fields because the $C_5$ and $C_6$ chemical shifts are sufficiently disparate (~14 ppm) to be independently refocused using shaped pulses. $C_6$ is a desirable observation site in systems with large $R_2$s because the presence of two $^1H$s cuts the delay required for transferring H-C antiphase magnetization into pure in-phase carbon magnetization (and vice-versa) in half. It

does, however, carry complications in interpretation due to the possible presence of internal motions about the $C_5$-$C_6$ bond.

Ring carbons do not carry the complication of additional bond rotations. Hence, $C_2$ was also a target for spin relaxation measurements. However, the Fc α1–6Man galactose ring resonances are especially sensitive to pulse sequence length; in fact, they are not observed in a sensitivity-enhanced carbon HSQC experiment, owing to additional refocusing delays before acquisition when compared to a standard phase-cycled HSQC experiment (data not shown). For this reason, combined with the larger $R_2$s, $^{13}C_2$ measurements were made, primarily, with direct carbon excitation / observation experiments using the same relaxation elements as those shown in Supplementary Figure 3. CPMG-type relaxation dispersion experiments were 1D $^{13}C_2$ excite/observe or $^{13}C_2$ excite/$^1$H observe using methods described27.

## Relaxation dispersion curve fitting

Relaxation dispersion data were fit with:

$$R_2(1/\tau_{CP}) = R_2^0 + \frac{\varphi_{EX}}{k_{EX}}\left(1 - \tanh(k_{EX}\tau_{CP}/2) \Big/ k_{EX}\tau_{CP}\right) \quad (1)$$

where

$$\varphi_{EX} = p_A p_B \Delta\omega^2 \quad (2)$$

$R_2^0$ is the relaxation rate in the absence of chemical exchange, $k_{EX}$ is the rate of exchange, $\tau_{CP}$ is the delay between refocusing pulses and Δωis the frequency difference of states A and B in angular units25.

## Chemical shift extraction from temperature dependencies

An equation to describe the chemical shift of a resonance in fast exchange at a given temperature in terms of enthalpy and entropy was derived by assuming two-state exchange between states A and B and temperature independent entropy and enthalpy values as shown in the Supplementary Methods section:

$$\delta_X = \delta_A - \frac{\delta_A - \delta_B}{\frac{1}{e^{-\left(\frac{1}{R}\right)\left(\frac{\Delta H}{T} - \Delta S\right)}} + 1} \quad (3)$$

Where $\delta_X$ is the observed chemical shift, $\delta_A$ and $\delta_B$ are the chemical shifts of states A and B, respectively, $R$ is the gas constant, $H$ is enthalpy, $S$ is entropy and $T$ is temperature.

## Calculation of $p_A$ using CPMG and chemical shift data

The population of the state A may be estimated using $\phi_{EX}$ and $\delta_A$:

$$p_A = \frac{1}{\frac{\omega_0^2(\delta_X - \delta_A)^2}{\varphi_{EX}} + 1} \quad (4)$$

where $\omega_o$ is the Larmor frequency of the nucleus in MHz. A derivation of this equation is presented in Supplementary Methods.

## Supplementary Material

Refer to Web version on PubMed Central for supplementary material.

## Acknowledgement

We thank Ting Yang and Prof. Maor Bar-Peled for the Galactokinase, Dr. Yizhou Liu for discussions of dynamics and pulse sequences, and Evan Brady for preparing the UDP-$^{13}C_U$-galactose. This research was funded by Grants from the NIH, R01GM033225 and P41RR005351. AWB was supported by a Kirschstein NRSA fellowship F32AR058084.

## References

1. Roitt, IM.; Brostoff, J.; Male, DK. Immunology. 6th ed.. New York: Mosby, Edinburgh; 2001.
2. Goronzy JJ, Weyand CM. Developments in the scientific understanding of rheumatoid arthritis. Arthritis Res Ther. 2009; 11:249. [PubMed: 19835638]
3. Arnold JN, et al. The impact of glycosylation on the biological function and structure of human immunoglobulins. Annual Review of Immunology. 2007; 25:21–50.
4. Alavi A, Axford JS. Sweet and sour: the impact of sugars on disease. Rheumatology. 2008; 47:760–770. [PubMed: 18375404]
5. Parekh RB, et al. Association of rheumatoid arthritis and primary osteoarthritis with changes in the glycosylation pattern of total serum IgG. Nature. 1985; 316:452–457. [PubMed: 3927174]
6. Kaneko Y, Nimmerjahn F, Madaio MP, Ravetch JV. Pathology and protection in nephrotoxic nephritis is determined by selective engagement of specific Fc receptors. Journal of Experimental Medicine. 2006; 203:789–797. [PubMed: 16520389]
7. Anthony RM, et al. Recapitulation of IVIG anti-inflammatory activity with a recombinant IgG Fc. Science. 2008; 320:373–376. [PubMed: 18420934]
8. Malhotra R, et al. Glycosylation changes of IgG associated with rheumatoid arthritis can activate complement via the mannose-binding protein. Nat Med. 1995; 1:237–243. [PubMed: 7585040]
9. Yamaguchi Y, et al. Glycoform-dependent conformational alteration of the Fc region of human immunoglobulin G1 as revealed by NMR spectroscopy. Biochimica Et Biophysica Acta-General Subjects. 2006; 1760:693–700.
10. Mimura Y, et al. Role of oligosaccharide residues of IgG1-Fc in Fc gamma RIIb binding. J Biol Chem. 2001; 276:45539–45547. [PubMed: 11567028]
11. Scallon BJ, et al. Higher levels of sialylated Fc glycans in immunoglobulin G molecules can adversely impact functionality. Mol Immunol. 2007; 44:1524–1534. [PubMed: 17045339]
12. Anthony RM, Wermeling F, Karlsson MC, Ravetch JV. Identification of a receptor required for the anti-inflammatory activity of IVIG. Proc Natl Acad Sci U S A. 2008; 105:19571–19578. [PubMed: 19036920]
13. Burmeister WP, Huber AH, Bjorkman PJ. Crystal structure of the complex of rat neonatal Fc receptor with Fc. Nature. 1994; 372:379–383. [PubMed: 7969498]
14. Sondermann P, Huber R, Oosthuizen V, Jacob U. The 3.2-A crystal structure of the human IgG1 Fc fragment-Fc gammaRIII complex. Nature. 2000; 406:267–273. [PubMed: 10917521]
15. Radaev S, et al. The structure of a human type III Fcgamma receptor in complex with Fc. J Biol Chem. 2001; 276:16469–16477. [PubMed: 11297532]
16. Idusogie EE, et al. Mapping of the C1q binding site on rituxan, a chimeric antibody with a human IgG1 Fc. J Immunol. 2000; 164:4178–4184. [PubMed: 10754313]
17. Deisenhofer J. Crystallographic refinement and atomic models of a human Fc fragment and its complex with fragment B of protein A from Staphylococcus aureus at 2.9- and 2.8-A resolution. Biochemistry-Us. 1981; 20:2361–2370.

18. Yamaguchi Y, et al. Dynamics of the carbohydrate chains attached to the Fc portion of immunoglobulin G as studied by NMR spectroscopy assisted by selective C-13 labeling of the glycans. J Biomol Nmr. 1998; 12:385–394. [PubMed: 9835046]
19. Wormald MR, et al. Variations in oligosaccharide-protein interactions in immunoglobulin G determine the site-specific glycosylation profiles and modulate the dynamic motion of the Fc oligosaccharides. Biochemistry-Us. 1997; 36:1370–1380.
20. Kobata A. The N-linked sugar chains of human immunoglobulin G: their unique pattern, and their functional roles. Biochim Biophys Acta. 2008; 1780:472–478. [PubMed: 17659840]
21. Barb AW, Brady EK, Prestegard JH. Branch-specific sialylation of IgG-Fc glycans by ST6Gal-I. Biochemistry-Us. 2009; 48:9705–9707.
22. Mittermaier A, Kay LE. New tools provide new insights in NMR studies of protein dynamics. Science. 2006; 312:224–228. [PubMed: 16614210]
23. Chang VT, et al. Glycoprotein structural genomics: solving the glycosylation problem. Structure. 2007; 15:267–273. [PubMed: 17355862]
24. Barb AW, et al. Intramolecular Glycan-Protein Interactions in Glycoproteins. Methods Enzymol. 2010; 477:365–388. [PubMed: 20816490]
25. Cavanagh, J. Protein NMR spectroscopy : principles and practice. 2nd ed.. Amsterdam ; Boston: Academic Press; 2007.
26. Palmer AG 3rd, Kroenke CD, Loria JP. Nuclear magnetic resonance methods for quantifying microsecond-to-millisecond motions in biological macromolecules. Methods Enzymol. 2001; 339:204–238. [PubMed: 11462813]
27. Hansen DF, et al. Probing chemical shifts of invisible states of proteins with relaxation dispersion NMR spectroscopy: How well can we do? J Am Chem Soc. 2008; 130:2667–2675. [PubMed: 18237174]
28. Raju TS. Terminal sugars of Fc glycans influence antibody effector functions of IgGs. Curr Opin Immunol. 2008; 20:471–478. [PubMed: 18606225]
29. Bock K, Pedersen C, Pedersen H. carbon-13 nuclear magnetic resonance data for oligosaccharides. Adv Carbohydr Chem Biochem. 1984; 42:193–225.
30. Wieruszeski JM, Michalski JC, Montreuil J, Strecker G. Sequential H-1 and C-13 Resonance Assignments for an Octasaccharide and Decasaccharide of the N-Acetyllactosamine Type by Multiple-Step Relayed Correlation and Hetero-Nuclear Correlation Nuclear Magnetic-Resonance. Glycoconjugate Journal. 1989; 6:183–194. [PubMed: 2535483]
31. Vliegenthart JFG, Dorland L, van Halbeek H. High-resolution, 1H-nuclear magnetic resonance spectroscopy as a tool in the structural analysis of carbohydrates related to glycoproteins. Adv Carbohydr Chem Biochem. 1983; 41:209–374.
32. Voynov V, et al. Dynamic fluctuations of protein-carbohydrate interactions promote protein aggregation. PLoS One. 2009; 4:e8425. [PubMed: 20037630]
33. Lipari G, Szabo A. Model-Free Approach to the Interpretation of Nuclear Magnetic-Resonance Relaxation in Macromolecules .1. Theory and Range of Validity. J Am Chem Soc. 1982; 104:4546–4559.
34. Lipari G, Szabo A. Model-Free Approach to the Interpretation of Nuclear Magnetic-Resonance Relaxation in Macromolecules .2. Analysis of Experimental Results. J Am Chem Soc. 1982; 104:4559–4570.
35. Raju TS, et al. Glycoengineering of therapeutic glycoproteins: in vitro galactosylation and sialylation of glycoproteins with terminal N-acetylglucosamine and galactose residues. Biochemistry-Us. 2001; 40:8868–8876.
36. Lund J, et al. Multiple interactions of IgG with its core oligosaccharide can modulate recognition by complement and human Fc gamma receptor I and influence the synthesis of its oligosaccharide chains. J Immunol. 1996; 157:4963–4969. [PubMed: 8943402]
37. DeLano WL, Ultsch MH, de Vos AM, Wells JA. Convergent solutions to binding at a protein-protein interface. Science. 2000; 287:1279–1283. [PubMed: 10678837]
38. Hirotsu K, Shimada A. Crystal and Molecular-Structure of Beta-Lactose. Bulletin of the Chemical Society of Japan. 1974; 47:1872–1879.

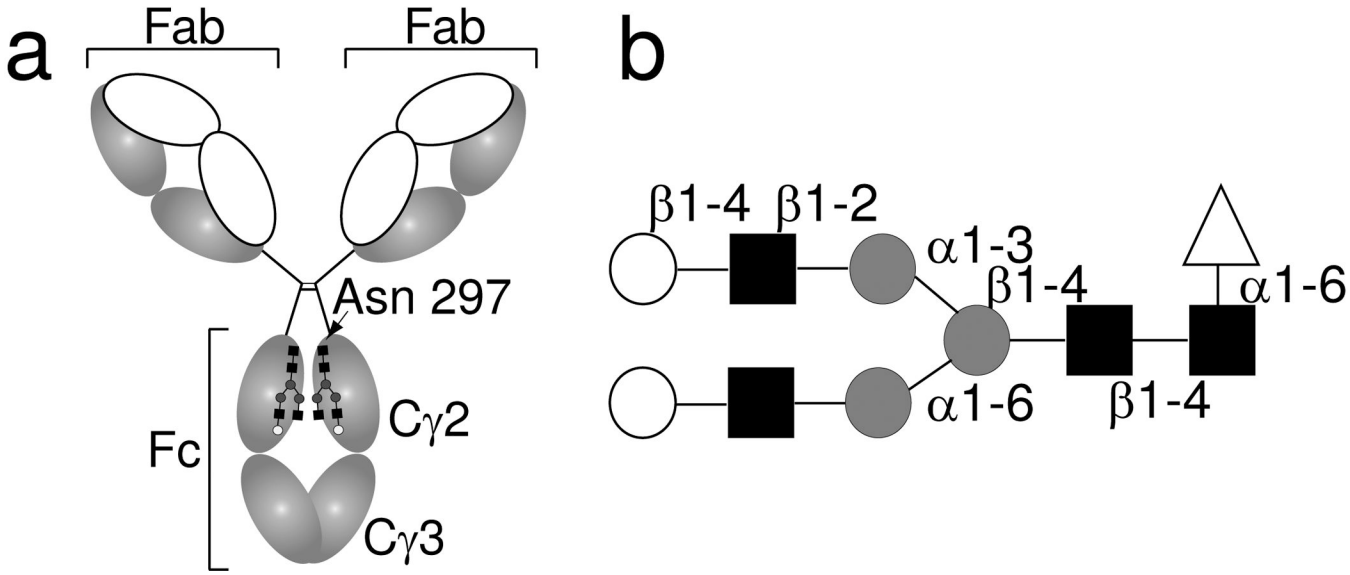


**Figure 1. Immunoglobulin G contains an N-linked glycan at Asn297**

(**a**) The domain organization of IgG1showing the antigen-binding Fab fragments, the Fc fragment, and the N-glycan. (**b**) The Fc glycan as remodeled in this work is predominantly a galactose-terminated complex-type, biantennary, fucosylated carbohydrate. *Open* circles indicate galactose, *filled* squares *N*-acetylglucosamine, *grey* circles mannose, and *open* triangles fucose residues.

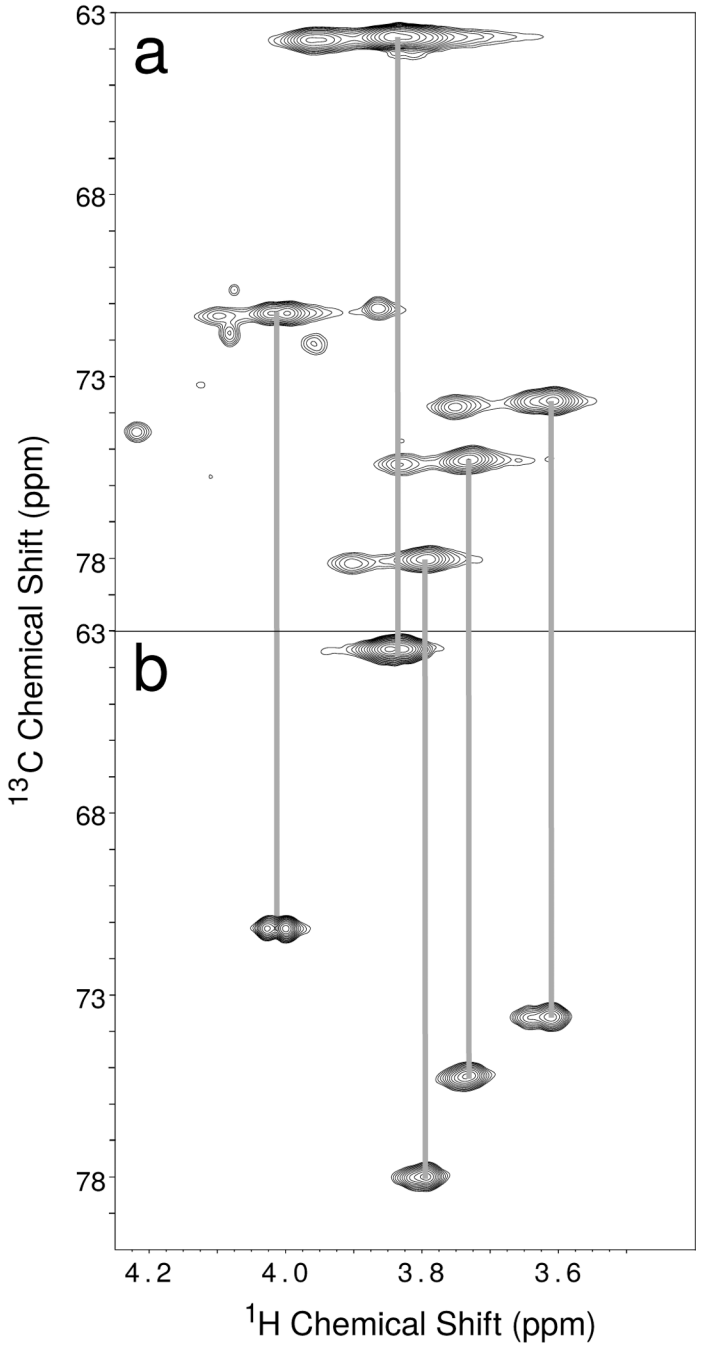


**Figure 2. A 2D $^{13}$C-$^{1}$H HMQC correlation spectrum of $^{13}$C-Galactose labeled IgG1 and IgG1 Fab fragment**

(**a**) IgG1 and (**b**) the IgG1 Fab fragment at 50°C. Vertical grey lines indicate resonances at the same $^{13}$C and $^{1}$H frequencies in both spectra.

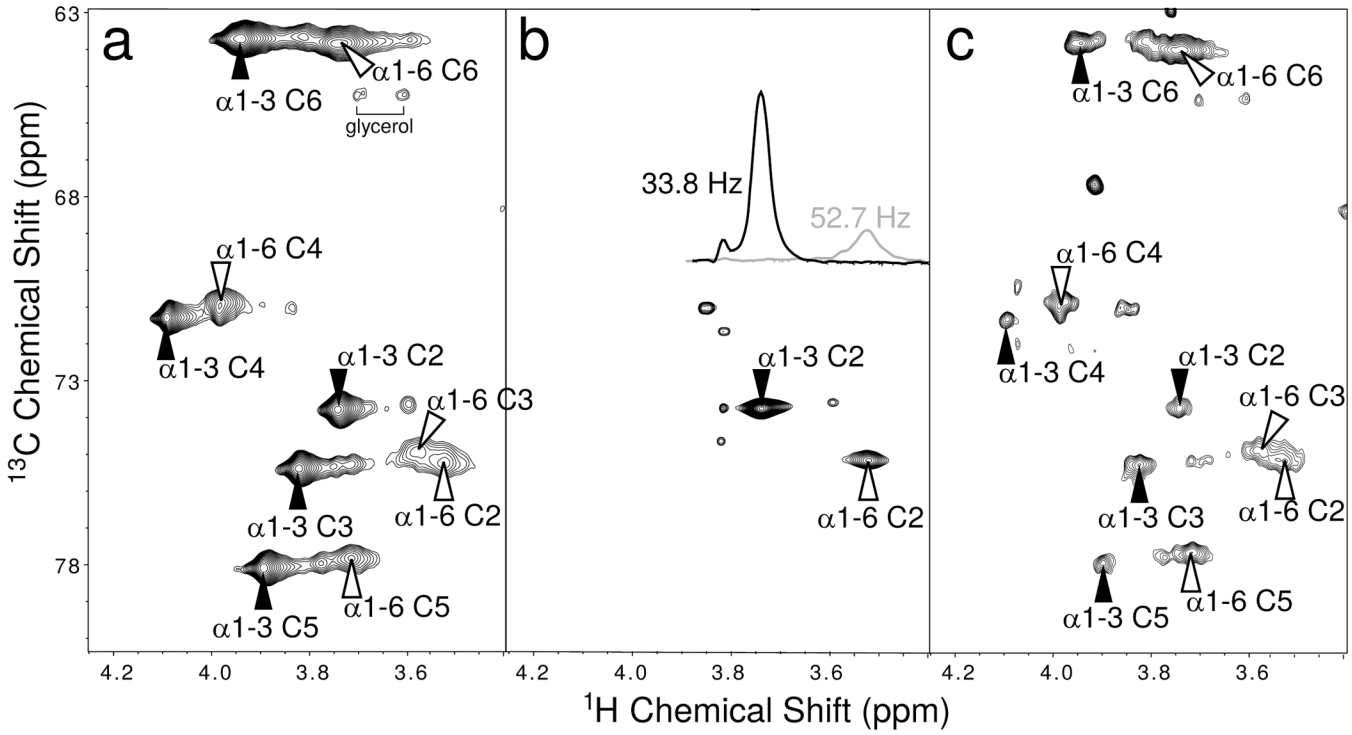


**Figure 3. 2D $^{13}$C-HMQC spectra and assignments of $^{13}$C-Galactose labeled IgG Fc**

(**a**) uniformly $^{13}$C-Galactose labeled Fc fragment and (**b**) $^{13}C_2$-Galactose labeled Fc fragment. The extracted lines show $^{1}$H linewidth measurements of the $H_2$-$C_2$ crosspeaks extracted from this spectrum. (**c**) IgG Fc fragment with the α1–6Man-linked Galactose enriched with $^{13}$C-Galactose. Filled (hollow) arrows denote a residue on the α1–3Manlinked (α1–6Man-linked) branch of the Fc-conjugated biantennary glycan. Anomeric peaks were overlapped with the residual HOD signal but were observed at lower temperatures.

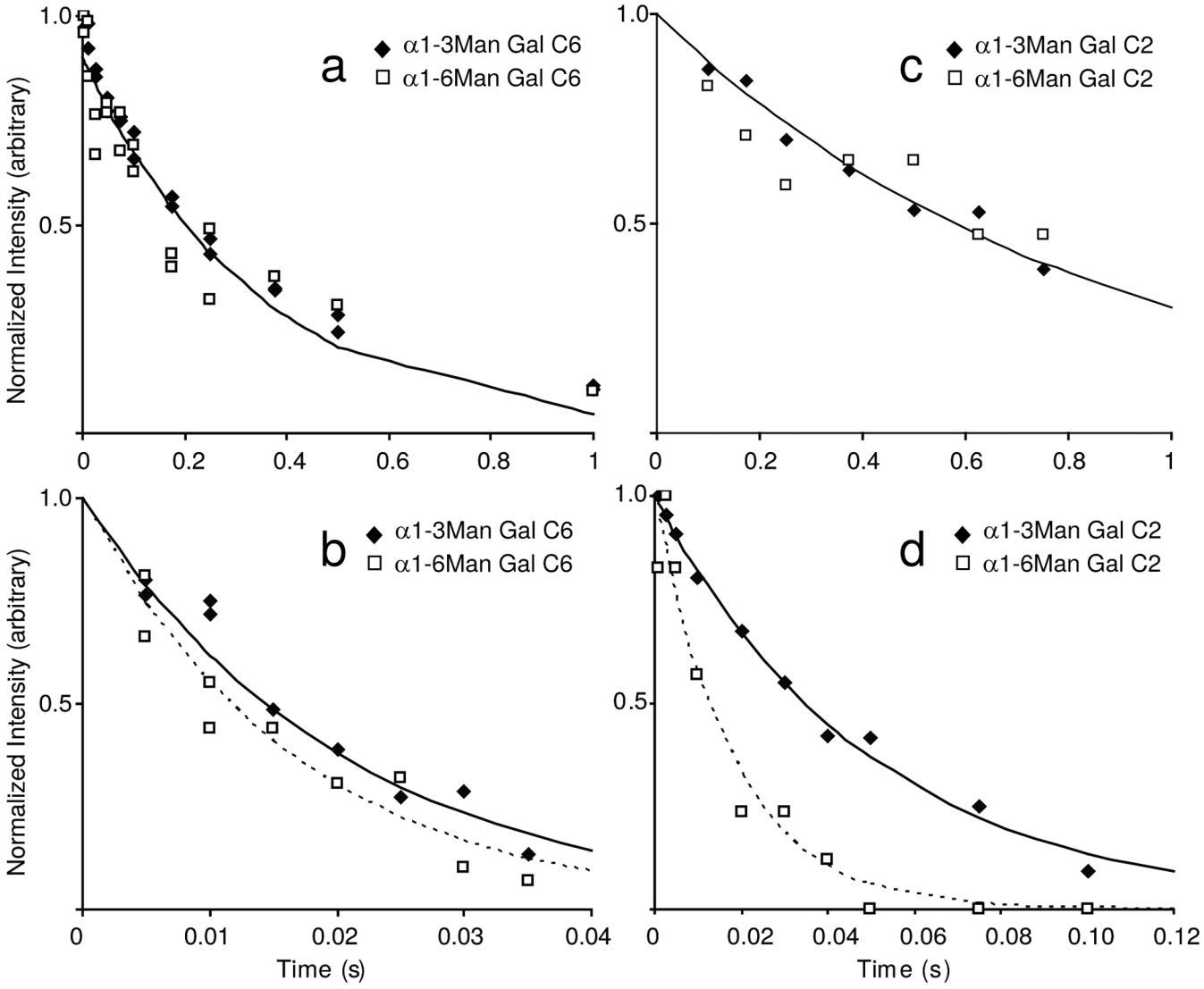


**Figure 4. $^{13}$C spin relaxation measurements of Galactose resonances**

(**a**) $R_1$ and (**b**) $R_2$ measurements of $^{13}C_6$. (**c**) $R_1$ and (**d**) $R_{1\rho}$ measurements of $^{13}C_2$. The data are fit with an equation describing a single exponential decay; using the rates shown in Table 1. Where the rates are significantly different, a solid (dashed) line denotes the α1–3Man-linked (α1–6Man-linked) fits. $R_{1\rho}$ measurements were obtained at an applied field strength of 5000Hz.

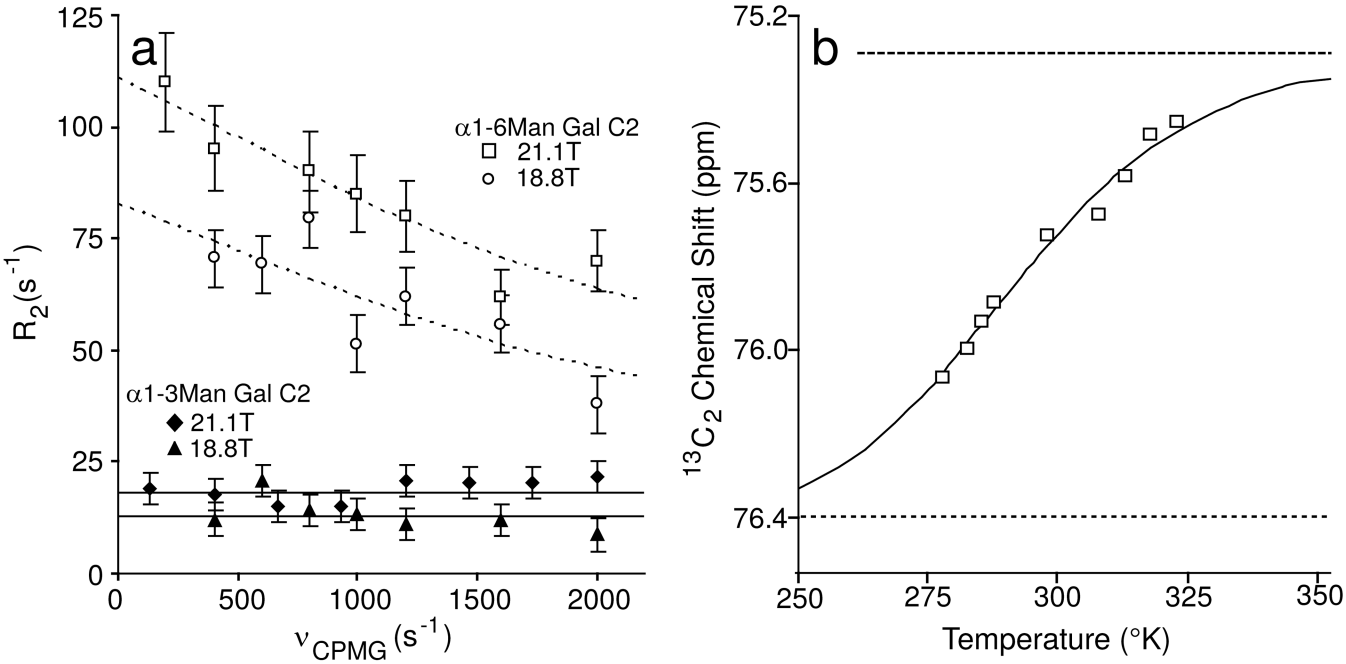


**Figure 5. Relaxation dispersion and temperature-dependent chemical shift measurements show evidence of two states**

Relaxation dispersion experiments (**a** reveal motion on a μs timescale for the α1–6Man-linked branch but not the α1–3Man-linked branch. When fitted to a two state model and data collected at three different magnetic fields, an exchange rate ($k_{EX}$) of 5300 ± 1700 $s^{-1}$ was estimated by fitting equation (1). (**b**) The chemical shift of the α1–6Man-linked $^{13}C_2$ resonance approaches a saturation point at high temperature and permits the estimation of chemical shift values for each of two states using Eq (3). Chemical shift asymptotes for the high temperature state A and low temperature state B are shown with dashed lines.

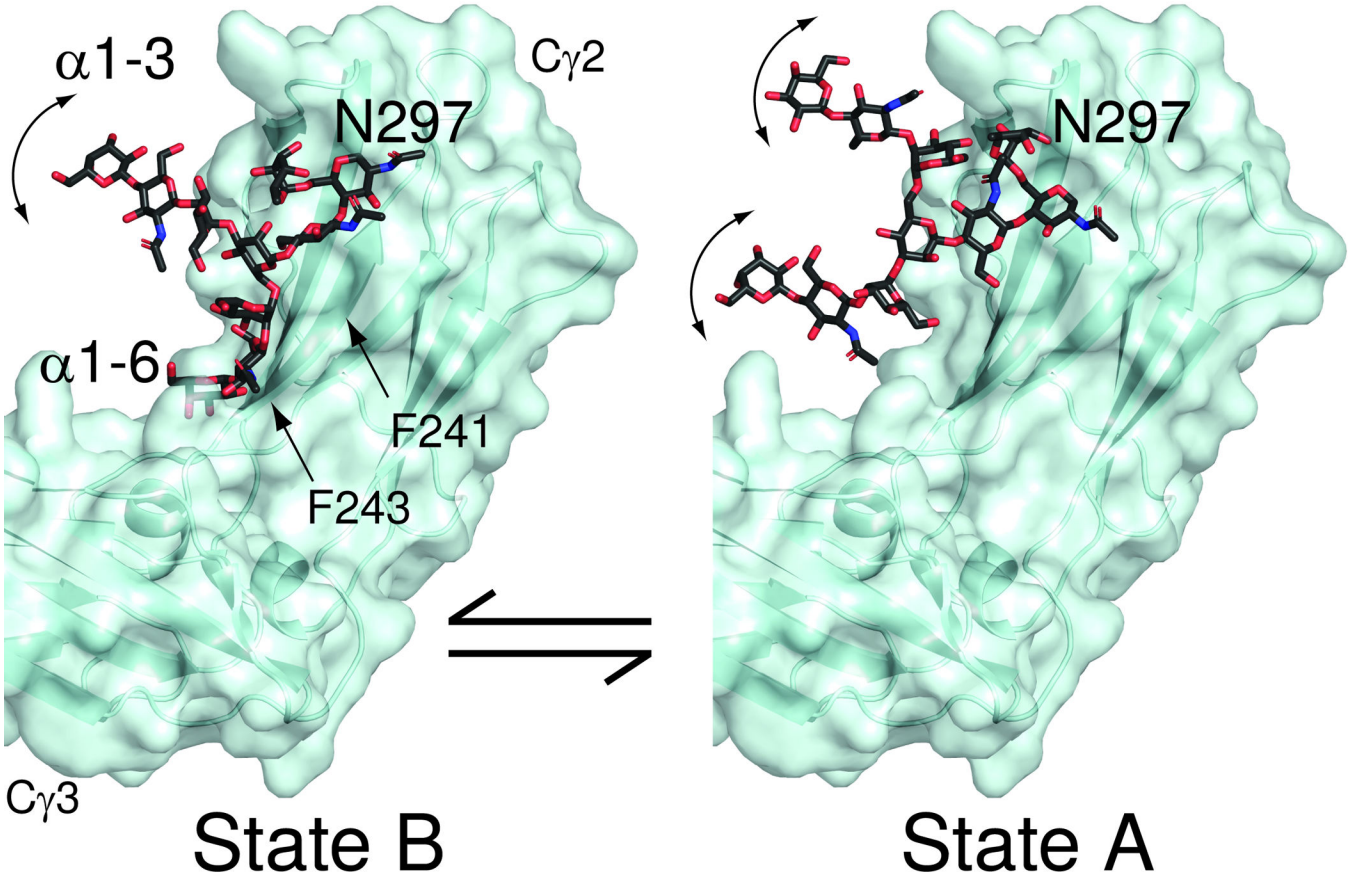


**Figure 6. Models for Fc glycan dynamics and accessibility showing exposed glycan conformations are possible**

The terminal galactose residues of the glycan are labeled as "α1–3"Man-linked or "α1–6"Man-linked. These hypothetical models show accessible locations of the glycans in states **A** and **B** based on X-ray structures of the Fc fragment (pdb-1l6x). State **B** is characterized by the α1–6Man-linked branch coordinated by the surface of the polypeptide, and both branches of state **A** are highly dynamic.

**Table 1**

$^{13}$C Gal-Fc Relaxation Measurements

| | α1–3Man-linked Relaxation Rates | α1–6Man-linked Relaxation Rates |
|---|---|---|
| **21.1T** | **Galactose $C_6$** | **Galactose $C_6$** |
| $R_1$ | 2.8 ± 0.1 $s^{-1}$ | 3.1 ± 0.4 $s^{-1}$ |
| $R_2$ | 48.4 ± 5.5 $s^{-1}$ | 59.7 ± 9.2 $s^{-1}$ |
| **21.1T** | **Galactose $C_2$** | **Galactose $C_2$** |
| $R_1$ | 1.2 ± 0.1 $s^{-1}$ | 1.2 ± 0.2 $s^{-1}$ |
| $R_{1\rho}$ | 20.1 ± 1.0 $s^{-1}$ | 56.1 ± 10 $s^{-1}$ |
| $R_2$ linewidth | 40 $s^{-1}$ | 150 $s^{-1}$ |
| **14.0T** | | |
| $R_{1\rho}$ | 14.7 ± 1.1 $s^{-1}$ | 48.0 ± 5.4 $s^{-1}$ |
| $R_2$ linewidth | 28 $s^{-1}$ | 107 $s^{-1}$ |
| $R_2$ | 29 $s^{-1}$ | n.d. |

n.d.- not determined due to low signal / noise

**Table 2**

Kinetic and Thermodynamic Parameters

| | |
|---|---|
| $k_{EX}$ | 5300 ± 1700 $s^{-1}$ |
| $\varphi_{EX}$ 21.1T | 380,000 ± 60,000 $rad^2$ $s^{-2}$ |
| $R_2^o$ 21.1T | 26 ± 13 $s^{-1}$ |
| $\varphi_{EX}$ 18.8T | 300,000 ± 100,000 $rad^2$ $s^{-2}$ |
| $R_2^o$ 18.8T | 39 ± 7 $s^{-1}$ |
| ΔH | 9.2 ± 0.6 kcal $mol^{-1}$ |
| ΔS | 0.032 ± 0.002 kcal $mol^{-1}$ $K^{-1}$ |
| $\delta_A$ | 75.3 ± 0.2 ppm |
| $\delta_B$[1] | 76.4 ± 0.5 ppm |
| $\delta_B$[2] | 76.4 ± 0.5 ppm |
| $\Delta\omega$[1] | 1600 rad $s^{-1}$ |
| $\Delta\omega$[2] | 1500 ± 300 rad $s^{-1}$ |

[1] values derived from chemical shift vs. T fit

[2] values derived from CPMG measurements